Model-based Control Approaches for Optimal Integration of a Hybrid Wind-diesel Power System in a Microgrid

Luis Ismael Minchala Avila[1,2], Adriana Vargas Martínez[2], Youmin Zhang[2],
Luis Eduardo Garza Castañón[1], Eduardo Robinson Calle Ortiz[3] and Julio César Viola[3]
[1]*Department of Mechatronics and Automation, Tec. de Monterrey, Eugenio Garza Sada 2501, Monterrey NL, Mexico*
[2]*Department of Mechanical and Industrial Engineering, Concordia University, 1455 de Maisonneuve, Montreal, Canada*
[3]*Engineering Research Center for Innovation and Development, Universidad Politécnica Salesiana, Calle Vieja 12-30, Cuenca, Ecuador*

Keywords: Distributed Generation, Hybrid Wind-diesel, Microgrids, Model Predictive Control, Model Reference Adaptive Control.

Abstract: This paper presents two model-based approaches for designing control strategies in order to integrate a diesel generator as frequency and voltage leader in an islanded microgrid configuration. The selected microgrid configuration is composed of a hybrid wind-diesel system with a battery storage system (BSS). A model predictive control (MPC) scheme and a model reference adaptive control (MRAC) scheme are selected for this task, due to its flexibility and capability for handling constraints and fault-tolerance, respectively, which is helpful for smart grid (SG) architectures to achieve reduced fuel consumption and with and enhanced reliability and integration of renewable energy sources (RES) into the electrical network. A constrained fuel consumption strategy has been implemented in the diesel engine generator (DEG) controller with the help of MPC strategy and fault-tolerance is achieved with MRAC. Different operating conditions of the microgrid were simulated: 1) diesel-only generation, 2) wind turbine generator (WTG) ignition, 3) sudden connection of 0.5 MW load, and 4) a 3-phase fault with duration of 0.5 seconds. Improved performance over a baseline controller, IEEE type 1 automatic voltage regulator (AVR), is achieved. Dynamic models of the network components are presented in details on design and implementation of the microgrid configuration in Matlab/Simulink®.

1 INTRODUCTION

Microgrids are small-scale low voltage power systems with distributed energy resources (DER), storage devices and controllable loads, connected to the main power network or islanded. Microgrids are concerned with power generation near the consumers (Jiang et al., 2009; Gentile, 2009). Nevertheless, microgrids have different operating characteristics than bulk power systems (BPS) such as lack of inertia, resistive lines and high penetration of RES.

Microgeneration units, typically located at users locations, have emerged as an option to meet growing customer needs for electric power with an emphasis on reliability, power quality, and contribution to different economic, environmental and technical benefits. The impact on power balance and grid frequency of microgeneration at low voltage levels, such as wind energy or photovoltaic (PV), is a great challenge (Schwaegerl et al., 2009). Wind is a promising RES due to its cleanness and social impact motivated by environmental and economical issues. However, wind energy also has some limiting characteristics such as: unschedulable, uncontrollable, etc. To obtain relatively constant power, variable blade pitch angle controls are installed in the wind turbines (WT) (Abdin and Xu, 2000; Abdal et al., 2010).

There is a variety of contributions on the field of simulating and controlling a hybrid wind-diesel power system. In (Vechiu et al., 2004; Kini and Yaragatti, 2006) detailed models of the system components of the hybrid configuration are presented, as well as performance analysis under different operating conditions, i.e. different wind velocities, load changes, etc., where IEEE type 1 AVR has been used. A fully distributed control strategy for a microgrid configuration integrating a WTG through DC-link voltage control is studied in (Vandoorn et al.,

Minchala Avila L., Vargas Martínez A., Zhang Y., Eduardo Garza Castañón L., Robinson Calle Ortiz E. and César Viola J..
Model-based Control Approaches for Optimal Integration of a Hybrid Wind-diesel Power System in a Microgrid.
DOI: 10.5220/0004359400120021
In *Proceedings of the 2nd International Conference on Smart Grids and Green IT Systems* (SMARTGREENS-2013), pages 12-21
ISBN: 978-989-8565-55-6

2011), where two loops control strategy (voltage and power) is designed and simulated for the WTG. In (Kassem and Ali, 2011) a robust control approach for long term operation of a hybrid wind-diesel system is presented, a linearized model of the entire system is proposed through the combination of the subsystem models, and it is used for the design of a centralized controller. A MPC strategy has been used for a stand-alone wind energy conversion system (WECS) in (Kassem, 2012) and a novel functional MPC is proposed for a faster processing time.

Frequency and voltage regulation in interconnected electrical systems with multiple sources generation are main control challenges in distributed generation systems. Many different approaches have been studied and proposed for both grid-connected and islanded microgrid operation. Grid-connected operation relies on main grid parameters and the majority of contributions are related with volt-var strategies through the use of capacitor banks and flexible AC transmission system (FACTS), although advanced control strategies like adaptive controllers for voltage regulation at the generation unit are detailed in (Fusco and Russo, 2008; Fusco and Russo, 2012). Islanded microgrid operation, on the other hand has generated the necessity of a frequency leader, or multiple frequency leaders under faulty scenarios, due to the high integration of RES whose intermittent characteristic complicates the use of traditional control schemes. Voltage and frequency regulation for isolated generators are studied in some research papers; in (Munoz-Aguilar et al., 2011) a sliding mode control for voltage amplitude regulation of a stand-alone synchronous generator connected to a resistive load is presented, while in (Kumar et al., 2008) a frequency regulator for a microgrid conformed by a diesel generator, a wind turbine power, an aqua electrolyzer and a fuel cell through multiple PI controllers is proposed. A multiagent-based automatic generation control (AGC) for isolated power systems with dispersed power sources such as PV, WTG, diesel generator and energy capacitor systems (ECS) for the energy storage is very well detailed in (Hiyama, 2011).

This paper presents the design methodology for controlling a hybrid wind-diesel system in islanded microgrid configuration using two model-based control approaches: MPC and MRAC. MPC is used for optimizing RES utilization and minimizing fuel consumption of the DEG with the help of MPC's optimized performance with constraints handling capabilities. MRAC is used for controlling the system under faulty scenarios due to its capability of adapting the control output for guaranteeing asymptotic output tracking. The control design objectives are to maintain desired voltage and frequency (frequency & voltage leader), and supply energy for the balanced load (total load - WTG power). With the model developed for each network component, a distributed control strategy is then proposed. Different operating conditions of the microgrid were simulated: 1) diesel-only generation, 2) wind turbine generator (WTG) ignition, 3) sudden connection of 0.5 MW load, and 4) a 3-phase fault with duration of 0.5 seconds. Improved performance over a baseline controller, IEEE type 1 AVR, is achieved.

The paper is organized as follows: Section II presents model generation of the microgrid components. Section III deals with the controllers design. Section IV presents simulation results and performance analysis and finally conclusions are drawn in Section V.

2 MODELING OF MICROGRID

A typical microgrid configuration, consists of DG units, controllable loads and storage. Fig. 1 presents a typical microgrid architecture, where it is remarkable the high penetration of RES and DC-links for integrating these intermitent units into the main grid. In the following subsections, detailed models of the network componentes are presented.

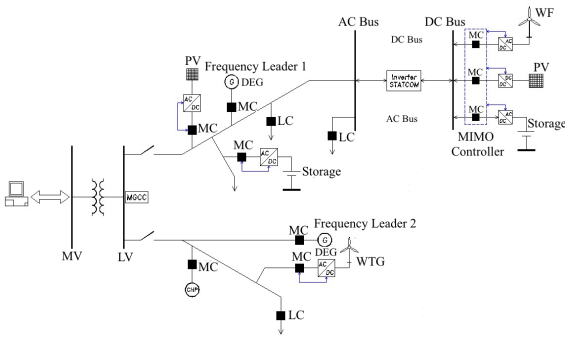

Figure 1: A typical microgrid architecture.

2.1 Diesel Engine Generator

The DEG is composed of two machines: diesel engine (prime mover) and synchronous generator. In the following two subsections the diesel engine and synchronous generator models are presented.

2.1.1 Diesel Engine

For a complete dynamic simulation of the diesel engine, a high order model would be required. However, for speed control purpose (frequency control of

the grid), a simpler model will be enough. Fig. 2 shows a block diagram of the diesel engine. The actuator block is modeled by a first-order system with a gain K_a and a time constant T_a. On the other hand, the diesel engine block contains the combustion system and it is responsible of the movement of the pistons and in consequence the crankshaft will generate a torque $T(s)$ in the shaft. Some research papers (Kuang et al., 2000; Lee et al., 2008) use a time delay $e^{-\tau s}$ and a torque constant K_b for modeling this block. The flywheel block is an approximation of the complex inertia dynamics generated inside the machine, while the ρ coefficient represents friction. The output, $x_2(t)$ represents the angular velocity of the machine's shaft. $d(s)$ is used for modeling load changes in rotor shaft, e.g. larger mechanical power demanded for the synchronous generator due to a connection of an electrical load.

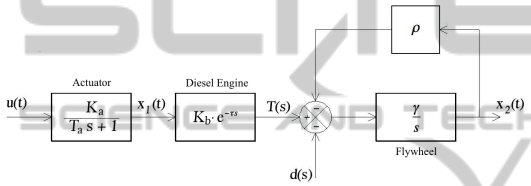

Figure 2: Classic diesel engine block diagram (Lee et al., 2008).

The continuous-time model of Fig. 2 is represented in state-space equations, as follows:

$$\dot{x}_1(t) = -\frac{1}{T_a}x_1(t) + \frac{K_a}{T_a}u(t) \quad (1)$$

$$\dot{x}_2(t) = \gamma K_b x_1(t-\tau) - \rho\gamma x_2(t) \quad (2)$$

$$\dot{\mathbf{x}}(t) = \mathbf{A}_0\mathbf{x}(t) + \mathbf{A}_1\mathbf{x}(t-\tau) + \mathbf{B}_0 u(t) \quad (3)$$

$$\mathbf{A}_0 = \begin{bmatrix} -\frac{1}{T_a} & 0 \\ 0 & -\rho\gamma \end{bmatrix} \quad (4)$$

$$\mathbf{A}_1 = \begin{bmatrix} 0 & 0 \\ \gamma K_b & 0 \end{bmatrix} \quad (5)$$

$$\mathbf{B}_0 = \begin{bmatrix} \frac{K_a}{T_a} \\ 0 \end{bmatrix} \quad (6)$$

System model (3) is a continuous time-delay state space representation that needs to be discretized for control design purposes. Many approaches for input-delay discretization has been proposed (Zeng and Hu, 2010), while a simpler solution is presented in (Jugo, 2002), which is adopted in this study. Characteristic values of the diesel engine constants in (3) are taken from (Kuang et al., 2000) and summarized in Table 1. Using a sampling time of 50 *ms*, one obtains:

$$\mathbf{x}[k+1] = \mathbf{x}[k] + \sum_{i=1}^{n_1} \frac{\left(\mathbf{A}_0 T_s + \mathbf{A}_1 T_s \mu\left(z^{-1}\right)\right)^i}{i!}\mathbf{x}[k] + \int_0^T \left(\frac{\left(\mathbf{A}_0 t + \mathbf{A}_1 t \mu\left(z^{-1}\right)\right)^i}{i!}\right)\mathbf{B}_0 dt\, u[k] \quad (7)$$

$$n_1 = 20;$$

$$\mathbf{x}[k+1] = \begin{bmatrix} 0.6703 & 0 \\ 0.0142 & 0.9985 \end{bmatrix}\mathbf{x}[k] + \begin{bmatrix} 0.3297 \\ 0.0030 \end{bmatrix} u[k] \quad (8)$$

Table 1: Typical parameters of a diesel engine.

System parameter	Value range	Nominal
Actuator gain K_a (pu)	1.0	1.0
Actuator time T_a (s)	$0.05 - 0.2$	0.125
Engine torque K_b (pu)	$0.8 - 1.5$	1.15
Engine dead time τ (s)	$0 - 1$	0.5
Plant. flywheel accel γ (s^{-1})	$0.1 - 0.5$	0.3
Friction coefficient ρ (pu)	0.1	0.1

2.1.2 Synchronous Generator

The machine's shaft is driven by a prime mover, i.e., steam, hydraulic turbine or diesel engine. The magnetic field produced by the field winding links the stator coils to induce voltage in the armature windings as the shaft is moved by the prime mover. A state-space model using the dynamic equations with dq (direct-quadrature) as frame reference, through a Park's transformation, for a pure resistive load R_L (a resistive load is used in the model, due to the fact that a microgrid is mainly resistive) connected into the synchronous machine is presented in (Munoz-Aguilar et al., 2011) and is summarized as following:

$$\mathbf{L}\frac{d\mathbf{x}}{dt} = \mathbf{A}\mathbf{x} + \mathbf{B}v_F \quad (9)$$

$$\mathbf{x} = \begin{bmatrix} i_d \\ i_q \\ i_F \end{bmatrix}$$

$$\mathbf{A} = \begin{bmatrix} -(R_s + R_L) & \omega L_s & 0 \\ -\omega L_s & -(R_s + R_L) & -\omega M_s \\ 0 & 0 & -R_F \end{bmatrix}$$

$$\mathbf{L} = \begin{bmatrix} L_s & 0 & M_s \\ 0 & L_s & 0 \\ M_s & 0 & L_F \end{bmatrix}$$

$$\mathbf{B} = \begin{bmatrix} 0 \\ 0 \\ 1 \end{bmatrix}$$

where $\begin{bmatrix} i_d & i_q & i_F \end{bmatrix}^T$ are the dq stator and field currents, respectively; R_s and R_F are the stator and

field resistances; L_s, L_m, and L_F are the stator, magnetizing, and field inductances; ω is the electrical speed; v_d and v_q are the dq stator voltages; and v_F is the field voltage which will be used as a control input. The parameters of the synchronous generator used for the simulation are: $Rs = 0.0036$, $L_m = 0.08$, $L_s = 0.057014$, $L_F = 0.1288$, $R_L = 0.5$, $\omega = 377$, $R_F = 39.65$.

2.2 Wind Turbine Generator

This subsection presents the model details of a WTG, where a horizontal-axis WT has been chosen as prime mover and an induction generator for energy conversion. This combination of WT and asynchronous machine is the most commonly WTG found in commercial versions for generating powers ranging from a few kilowatts up to 3 MW. The operating condition of the wind turbine is classified into three regimes: startup regime, sub-rated power regime and rated power regime. Dynamic simulation and the controller design are investigated in this work at rated power regime.

2.2.1 Wind Turbine Model

A WT model has been proposed in (Abdin and Xu, 2000; Abdal et al., 2010), where a PID algorithm for blade pitch control is mainly used. The WT model that will be used here is a lumped mass one, i.e. it does not model the double mass phenomenon. The turbine is pitch controlled through the blade pitch angle, β. The power coefficient, C_p characterizes the WT which is function of both tip speed ratio, $\lambda = \frac{\Omega R}{V_w}$ and β, where R is the wind turbine rotor radius, Ω is the mechanical angular velocity of the WT rotor and V_w is the wind velocity.

$$C_p(\lambda,\beta) = \left[116\left(\frac{1}{\lambda+0.08\beta} - \frac{0.035}{\beta^3+1}\right) - 0.4\beta - 5\right] \times 0.5716e^{-21\left(\frac{1}{\lambda+0.08\beta} - \frac{0.035}{\beta^3+1}\right)} + 0.0039\lambda \quad (10)$$

The dynamic output is the mechanical torque (T_m) of the WT and is expressed as:

$$T_m = \frac{\rho A R C_p V_w^2}{2\lambda} \quad (11)$$

where ρ is the air density and A represents the swept area by the blades.

2.2.2 Induction Generator

The electrical equations of induction generator model in the dq reference frame can be expressed as:

$$v_{qs} = r_s i_{qs} + \frac{\omega}{\omega_b}\psi_{ds} + \frac{p}{\omega_b}\psi_{qs} \quad (12)$$

$$v_{ds} = r_s i_{ds} - \frac{\omega}{\omega_b}\psi_{qs} + \frac{p}{\omega_b}\psi_{ds} \quad (13)$$

$$v'_{qr} = r'_r i'_{qr} + \left(\frac{\omega-\omega_r}{\omega_b}\right)\psi'_{dr} + \frac{p}{\omega_b}\psi'_{qr} \quad (14)$$

$$v'_{dr} = r'_r i'_{dr} + \left(\frac{\omega-\omega_r}{\omega_b}\right)\psi'_{qr} + \frac{p}{\omega_b}\psi'_{dr} \quad (15)$$

where ω_b is the base electrical angular velocity used to calculate the inductive reactances. The mechanical part is expressed in per unit as:

$$\frac{p}{\omega_b}\omega_r = \frac{1}{2H}(T_e - T_m) \quad (16)$$

$$T_e = \psi'_{qr} i'_{dr} - \psi'_{dr} i'_{qr} \quad (17)$$

2.3 Storage Subsystem

An electrical battery is one or more electrochemical cells that convert stored chemical energy into electrical energy. Lead-acid batteries are fully charged if one can measure an open-circuit voltage of fully discharged battery cell(s). The term discharged means that all free charges within the battery are zero and the only voltage source is the cell(s) voltage, V_0 (Fuchs and Masoum, 2011).

A simple nonlinear Thevenin model has been adopted for mathematical modeling purpose in (Chiasson and Vairamohan, 2005), whose aim is to design a discrete time estimator for the state of charge (SOC) of the battery. This model takes into account the dynamic response of the battery, which is influenced by the capacitive effects of the battery plates and by the charge-transfer resistance. Fig. 3 shows the equivalent circuit.

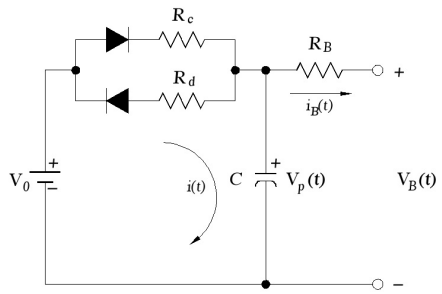

Figure 3: Equivalent circuit of lead-acid battery.

In order to design control strategies for charge and discharge process of the battery, it is required to define state space equations, leading to the following equations for the discharge process (charge process is similar, except for using R_c instead of R_d):

$$V_0 = R_d i(t) + \frac{1}{C}\int [i(t) + i_B(t)]\,dt$$

$$V_p(t) = \frac{1}{C}\int [i(t) + i_B(t)]\,dt$$

$$V_0 = R_d C\frac{dV_p(t)}{dt} + \frac{1}{C}i_B(t) + \frac{1}{R_d C}V_0 \quad (18)$$

$$\frac{dV_p(t)}{dt} = -\frac{1}{R_d C}V_p(t) - \frac{1}{C}i_B(t) + \frac{1}{R_d C}V_0 \quad (19)$$

$$V_B(t) = V_p(t) - R_B i_B(t) \quad (20)$$

A linear (approximate) relationship between open circuit voltage and SOC is used in several research papers (Chiasson and Vairamohan, 2005; Carter et al., 2012), leading to a simple equation for estimating battery's SOC:

$$S(t) = \frac{v_{oc}(t) - b}{a} \quad (21)$$

where b is the battery terminal voltage when $S(t) = 0\%$ and a is obtained knowing the value of b and v_{oc} at $SOC = 100\%$.

3 CONTROLLERS DESIGN

Figure 4 depicts the hybrid wind-diesel power system architecture that has to be controlled, where DC stands for distributed controller, CB stands for circuit breaker and ILVDCB for intelligent low voltage dc breaker (Minchala et al., 2012). The proposed control strategy is composed of three distributed controllers, each one with specific tasks:

1. *DC1* implements two non-decoupled MPCs as a first approach and two MRACs as a second approach that are in charge of regulating both grid frequency and voltage amplitude. A diesel engine is used as a prime mover which drags a synchronous machine generator at a constant speed. In an islanded configuration, the frequency is determined by the mechanical speed ω_m which is provided by the diesel engine, while the voltage amplitude is set by the synchronous generator field voltage.
2. *DC2* is regarded with power generation control of the WTG. In this first stage of investigation, an unconstrained MPC for a limited range of the blade pitch angle, β between 0 to 10 degrees, has been designed.
3. *DC3* controls a bi-directional dc−dc converter to manage battery charge and discharge. A classic PWM modulation control for the boost and buck converters is used.

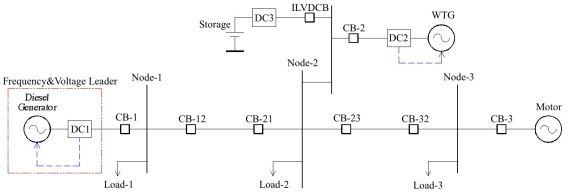

Figure 4: Hybrid wind-diesel power system architecture.

3.1 MPC Design

An integrator for reducing the steady-state error in closed-loop has been added to MPC designs. The augmented state-space model for diesel engine, SM and WTG can be obtained as follows (Wang, 2009):

$$\mathbf{x}_m(k+1) = \mathbf{A}_m\mathbf{x}_m(k) + \mathbf{B}_m u(k) \quad (22)$$

$$\mathbf{y}(k) = \mathbf{C}_m\mathbf{x}_m(k) \quad (23)$$

$$\Delta\mathbf{x}_m(k+1) = \mathbf{A}_m\Delta\mathbf{x}_m(k) + \mathbf{B}_m\Delta u(k) \quad (24)$$

$$\Delta\mathbf{x}_m(k) = \mathbf{x}_m(k) - \mathbf{x}_m(k-1) \quad (25)$$

$$\Delta u(k) = u(k) - u(k-1) \quad (26)$$

$$\mathbf{x}(k+1) = \mathbf{A}\mathbf{x} + \mathbf{B}\Delta u(k) \quad (27)$$

$$\mathbf{x}(k) = \begin{bmatrix} \Delta\mathbf{x}_m(k+1) \\ \mathbf{y}(k+1) \end{bmatrix} \quad (28)$$

$$\mathbf{A} = \begin{bmatrix} \mathbf{A}_m & \mathbf{0}_m^T \\ \mathbf{C}_m\mathbf{A}_m & \mathbf{1} \end{bmatrix} \quad (29)$$

$$\mathbf{B} = \begin{bmatrix} \mathbf{B}_m \\ \mathbf{C}_m\mathbf{B}_m \end{bmatrix} \quad (30)$$

$$\mathbf{y}(k) = \begin{bmatrix} \mathbf{0}_m & 1 \end{bmatrix}\mathbf{x}(k) \quad (31)$$

where $\mathbf{A}_m$, $\mathbf{B}_m$, $\mathbf{C}_m$ and $\mathbf{x}_m$ represent the state matrix, input matrix, output matrix and state vector of the model, respectively. The augmented model in state space that includes the integrator is represented by $\mathbf{A}$, $\mathbf{B}$, $\mathbf{x}$ and Δu. MPC uses this explicit model to predict future trajectories of system states and outputs. This prediction capability allows to solve optimal control problems online, where prediction error and control input action are minimized over a prediction horizon, N_p. The optimization yields to an optimal control sequence as input and only the first element from the sequence is used as the control signal for controlling the system, while the whole optimization procedure is repeated over and over again in each sampling step. The final aim of MPC is to provide zero output tracking error with minimal control effort. Designing a MPC with constraints is equivalent to solving a quadratic programming problem in order to find the parameter vector $\Delta\mathbf{U}$, which minimizes a cost function J subject to inequality constraints as follows:

$$\begin{aligned} J &= [\mathbf{R}_s - \mathbf{F}\mathbf{x}(k_i)]^T - 2\Delta\mathbf{U}^T\Phi^T[\mathbf{R}_s - \mathbf{F}\mathbf{x}(k_i)] \\ &+ \Delta\mathbf{U}^T\left(\Phi^T\Phi + \mathbf{R}\right)\Delta\mathbf{U} \quad (32) \\ \gamma &\geq \mathbf{M}\Delta\mathbf{U} \quad (33) \\ u(k) &= u(k-1) + \Delta u(k) \quad (34) \\ \mathbf{F} &= \begin{bmatrix} \mathbf{CA} & \mathbf{CA^2} & \mathbf{CA^3} & \cdots & \mathbf{CA^{N_p}} \end{bmatrix}^T \quad (35) \end{aligned}$$

$$\Phi = \begin{bmatrix} \mathbf{CB} & \mathbf{0} & \cdots & \mathbf{0} \\ \mathbf{CAB} & \mathbf{CB} & \cdots & \mathbf{0} \\ \mathbf{CA^2B} & \mathbf{CAB} & \cdots & \mathbf{0} \\ \vdots & \vdots & \vdots & \vdots \\ \mathbf{CA}^{N_p-1}\mathbf{B} & \mathbf{CA}^{N_p-2}\mathbf{B} & \cdots & \mathbf{CA}^{N_p-N_c}\mathbf{B} \end{bmatrix} \quad (36)$$

where $\mathbf{R} = r_w\mathbf{I}_{N_c\times N_c}$ and r_w is used as a tuning parameter for the desired closed-loop performance. $\mathbf{R}_s$ is a vector with length N_p that allows a comparison between reference signal and model output, for which case we assume that the reference, $r(k)$ is constant in the prediction horizon. $\mathbf{M} \in \mathbb{R}^{(2N_p+4N_c)\times N_c}$ and $\gamma \in \mathbb{R}^{(2N_p+4N_c)\times 1}$ are adequate matrices that represent every constraint in matrix form. Hildreth's quadratic programming algorithm has been used for updating control law, whose processing time in every sampling interval varies from less than 1 ms up to 35 ms (*tic toc* instruction in Matlab), for a computer with an i7 2.3 GHz processor and 4 GB of RAM memory.

The following design parameters have been adopted in the controllers:

- *SM rotor speed controller:* One of the aims of the optimal integration of the diesel generator in the microgrid is to reduce fuel consumption, giving priority to the power coming from RES, in our case from WTG. To achieve this objective, a hard constraint on the control signal is imposed, although softening this constraint will allow a better performance as it will be shown in the simulation results. The maximum tolerable frequency deviation is ± 3 and a hard constraint for y is imposed according to this and finally neither accelerations nor deaccelerations greater than 50% are allowed and a constraint for this requirement is also considered.

$$\begin{aligned} N_p &= 20 \\ N_c &= 10 \\ r_w &= 20 \\ 0 &\leq u \leq 0.8 \\ -0.5 &\leq \Delta u \leq 0.5 \\ 0.97 &\leq y \leq 1.03 \end{aligned}$$

- *SM Voltage Output Controller.* Due to a resistive load has been considered in (9), a greater prediction horizon than the preceding controller is considered, in order to assure system stability when capacitive and inductive loads are connected into the system. The only hard constraint is on the control signal, since it is not admissible to have values smaller than zero and greater than 2 in order to avoid saturation phenomenoms in the SM magnetic circuit.

$$\begin{aligned} N_p &= 50 \\ N_c &= 5 \\ r_w &= 5 \\ 0 &\leq u \leq 2 \end{aligned}$$

- *WTG Power Controller.* An unconstrained controller for a pitch angle range from 0 to 10 degrees is used. A stable behaviour is reached out of this range with this controller, although a degraded performance on settling time is obtained, due to the nonlinear relationship between β and generated power.

$$\begin{aligned} N_p &= 20 \\ N_c &= 10 \\ r_w &= 0.7 \end{aligned}$$

3.2 MRAC Design

The MRAC implements a closed-loop controller that involves the parameters that should be optimized, in order to modify the system response to achieve the desired final value. The adaptation mechanism adjusts the controller parameters to match the process output with the reference model output. The reference model is specified as the ideal model behavior that the system is expected to follow. The design approach chosen for this work is the one using the Lyapunov theory, presented in (Astrom and Wittenmark, 1995) and adapted here:

$$e = y_{process} - y_{reference} = G_p \times u - G_{ref} \times u_c \quad (37)$$

where e, $y_{process}$, $y_{reference}$, G_p, u, G_{ref} and u_c represent the error, process output, reference output, process model, process input, reference model and controller signal, respectively. For a second order system, the implemented MRAC scheme has two adaptation parameters: adaptive feedfoward gain θ_1 and adaptive feedback gain θ_2 . These parameters will be updated to follow the reference model. Then, the input is rewritten in terms of the adaptive feedforward and adaptive feedback gains as follows:

$$u = \theta_1 \times u_c - \theta_2 \times y_{process} \tag{38}$$

The Lyapunov stability theorem establishes the following: If there exists a function $V : R_n \rightarrow R$ being positive definite and its derivative:

$$\frac{dV}{dT} = \frac{\partial V^T}{\partial x}\frac{dx}{dt} = \frac{\partial V^T}{\partial x} f(x) = -W(x) \tag{39}$$

is negative semidefinite, then the solution $x(t) = 0$ to

$$\frac{dx}{dt} = f(x) \quad f(0) = 0 \tag{40}$$

is stable. If $\frac{dV}{dt}$ is negative definite the solution will be asymptotically stable. V denotes the Lyapunov function for the system. If

$$\frac{dV}{dt} < 0 \ \ and \ \ V(x) \rightarrow \infty \ \ when \ \ ||x|| \rightarrow \infty \tag{41}$$

the solution is globally asymptotically stable.

To design an MRAC controller using Lyapunov theory, the first step is to derive a differential equation for the error that contains the adaptation parameters. Then, a Lyapunov function and an adaptation mechanism need to be established to reduce the error to zero. The Lyapunov derivative function $\frac{dV}{dt}$ is usually negative semidefinite. Therefore, determining the parameter convergence is necessary to establish persistently excitation and uniform observability on the system and the reference signal (Nagrath and Gopal, 2008). The proposed Lyapunov function is quadratic in tracking error and controller parameter estimation error because it is expected that the adaptation mechanism will drive both types of errors to zero. From the equation error dynamics (42) the proposed Lyapunov function can be chosen as (43):

$$\frac{de}{dt} = -\frac{1}{a_{1r}}\frac{d^2e}{dt^2} - \frac{a_{0r}}{a_{1r}}e + \frac{b_r}{a_{1r}}(\theta_1 - 1)u_c - \frac{b_r}{a_{1r}}\theta_2 y_p \tag{42}$$

$$V(e,\theta_1,\theta_2) = \frac{1}{2}\left(a_{1r}e^2 + \frac{b_r}{\gamma}(\theta_1 - 1)^2 + \frac{b_r}{\gamma}(\theta_2)^2\right) \tag{43}$$

where b_r, γ and $a_{1r} > 0$.

Equation (43) will be zero when the error is zero and the controller parameters are equal to the desired values. The above Lyapunov function is valid if the derivative of this function is negative. Thus, the derivative of (44) is:

$$\dot{V} = a_{1r}e\frac{de}{dt} + \frac{b_r}{\gamma}(\theta_1 - 1)\frac{d\theta_1}{dt}\frac{b_r}{\gamma}\theta_2\frac{d\theta_2}{dt} \tag{44}$$

Substituting (42) in the above equation and rearranging the similar terms, equation (45) is obtained:

$$\begin{aligned}\dot{V} \ &= \ -e\frac{d^2e}{dt^2} - a_{0r}e^2 + \frac{1}{\gamma}(b_r\theta_1 - b_r)\left(\frac{d\theta_1}{dt} + \gamma u_c e\right) \\ &+ \ \frac{1}{\gamma}(b_r\theta_2)\left(\frac{d\theta_2}{dt} - \gamma y_{process}e\right)\end{aligned} \tag{45}$$

If the adaptation parameters are updated as:

$$\frac{d\theta_1}{dt} = -\gamma u_c e \ \ \text{and} \ \ \frac{d\theta_2}{dt} = \gamma y_{process}e \tag{46}$$

then,

$$\dot{V} = -e\frac{d^2e}{dt^2} - a_{0r}e^2 \tag{47}$$

It can be seen that (47) is negative semidefinite which implies $V(t) \leq V(0)$. This ensures that e, θ_1 and θ_2 are bounded. Since $a_{1r} > 0$, $a_{0r} > 0$ and u_c is bounded then $y_{reference}$ is bounded and therefore $y_{process} = e + y_{reference}$ is bounded as well. From the boundedness and convergence set theorem it can be concluded that the error e will go to zero (Nagrath and Gopal, 2008).

To overcome the limitations of the simple MRAC structure (smaller fault accommodation threshold than the MRAC in combination with other structures), a classical PID controller expressed in the form

$$PID = K_p + \frac{K_i}{s} + K_d s \tag{48}$$

is introduced in the feedforward part of the simple MRAC scheme. The PID parameters were obtained by using a genetic algorithm pattern search to track the desired system trajectory with the Matlab® Optimization Toolbox. The desired closed-loop behavior of the system is established through the model reference trajectory when there is no fault in the system. The parameters that need to be established for the desired optimization are shown in Table 2.

Table 2: Matlab® Optimization Toolbox parameters.

Parameters	Value
Step initial value	0
Step final value	1
Step time	0
Rise time	6s
% Rise	90
Settling time	9s
% Settling	5
% Overshoot	20
% Undershoot	2

Then, the genetic algorithm (GA) obtains the best parameter optimization (see Table 3). The desired response is introduced in terms of rise time, stabilization time and overshoots.

Table 3: Optimized PID parameters using GA.

Parameter	PID
K_p	3.8748
K_i	2.6471
K_d	1.9347

The MRAC has an adaptation learning rate $\gamma = 0.99$ for simulations to be presented in next section.

4 SIMULATION RESULTS

The system architecture shown in Fig. 4 was implemented in Matlab/Simulink®. System parameters are shown in Table 4. Three different controllers for the diesel engine generator were tested, the first one is the baseline diesel engine speed and voltage control that Matlab has in its library, i.e. governor and PI controller for the rotor speed control and IEEE type 1 AVR for maintaining the voltage amplitude of the microgrid. The second control approach tested is the MPC described in sub-section 3.1 and the third one is the MRAC described in sub-section 3.2. Variable wind speed was used during the simulation, whose velocity in every time instant of the simulation is depicted in Fig. 5.

Table 4: Hybrid wind-diesel system parameters.

Parameter	Value
SM power	3 MVA
Grid voltage	220 V
Grid frequency	60 Hz
WT nominal mechanical output	1.5 MW
WT max power at base wind speed	0.85
Base wind speed	12 m/s
Load-1	2 MW
Load-2	0.5 MW
Load-3	0.4 MW

Fig. 6 shows the simulation results when the MPC with softened constraint is used and Fig. 7 shows the simulation results for the three control approaches. The exact same events were tested in every case: (i) when system is in steady state and WTG is off, then suddenly WTG is turned on (after 12 seconds have elapsed in the simulation) and the battery starts charging from 50% of SOC; (ii) when 50 seconds have

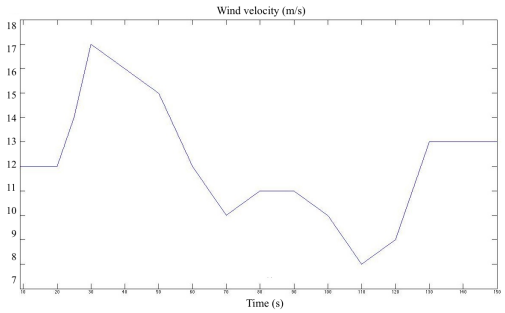

Figure 5: Wind velocity during the simulation.

elapsed, Load-2 is connected whose power consumption is 0.5 MW; and (iii) a three-phase fault of 0.5 s of duration is present in node-3 when 100 s of the simulation time have elapsed. CB-32 disconnects everything that is at its right side for isolating the fault. MPC and MRAC show a much better performance than the baseline controller and also they offer several advantages over it, as summarized in Table 5.

Table 5: Advantages of MPC and MRAC over classic controllers for DG integration in the microgrids.

	Robustness	Fault-Tolerance	Constraints Management	Scalability
MPC	High	Yes	Yes	High
MRAC	Very High	Yes	No	High
Classic control	Low	No	No	Low

A maximum power extraction from the WTG is pretended by this network configuration through pitch angle control by a PID controller when the baseline controller is used and unconstrained MPC when MPC and MRAC are used in the diesel generator. Different wind speeds are present, so 1 MW of power reference is set in the WTG, and the balanced load (total load - WTG power) is fed by the diesel engine. Battery is charging from its initial SOC until full and is being fed by an ac to dc converter with PWM control, whose duty cycle has been set to 1.

5 CONCLUSIONS

A distributed MPC strategy and a MRAC with a PID controller whose parameters were tuned using a GA have been developed in this paper for an islanded microgrid configuration which integrates the wind turbine generator and diesel engine generator for more efficient electricity generation in the framework of smart grids. Compared with a baseline controller, the

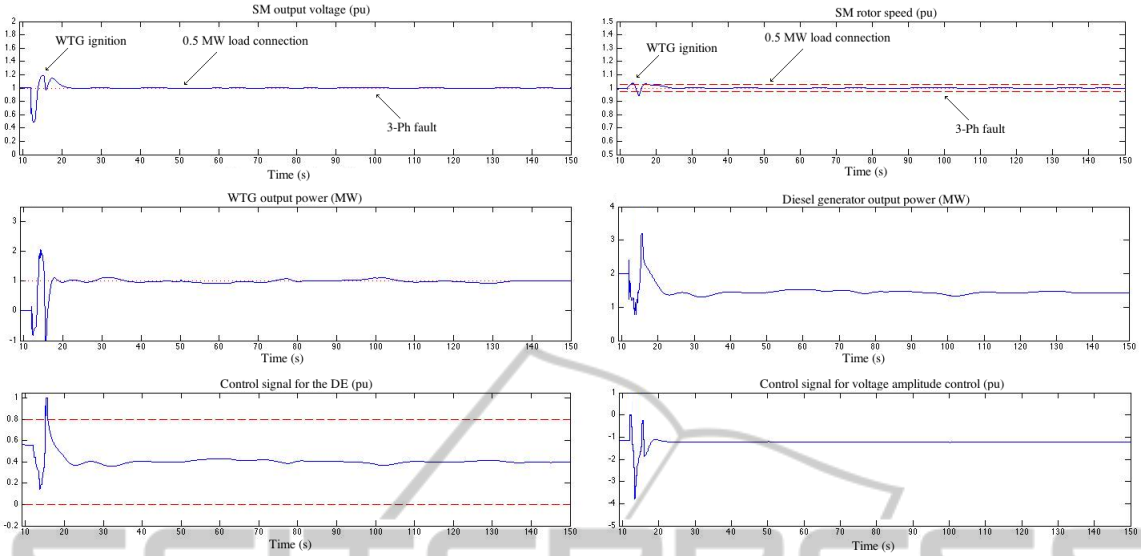

Figure 6: System simulation with MPC controlling the diesel generator and the WTG.

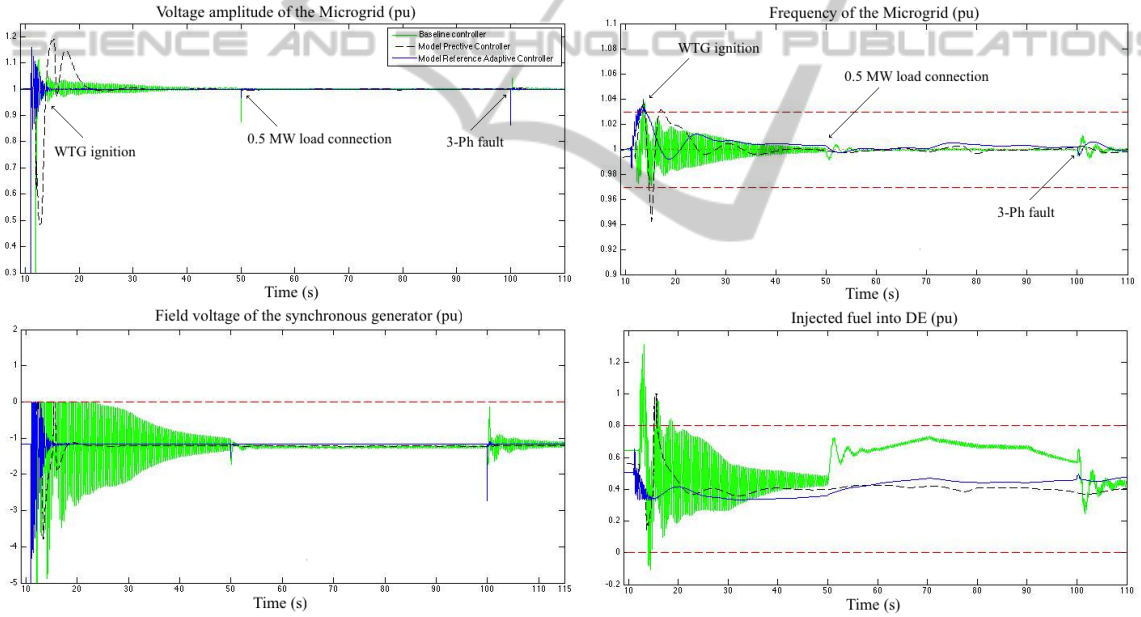

Figure 7: Performance comparison for the three different control approaches.

developed controllers, MPC and MRAC, achieved a better performance in both voltage and frequency responses. Softening the control signal constraint of the diesel engine during WT ignition offered an improved response in frequency control. Hard constraint on the control signal of the diesel engine allows setting maximum fuel consumption and prioritizes energy generated by RES. A major advantage of MPC is its ability to integrate constraints in the design that can be used in a future work for FTC capabilities. On the other hand the MRAC has an inherent capacity to accommodate perturbations and faults and direct physical interpretation, and it is relative easy for implementation. However, the use of only this type of controller has certain limitations. For this reason, it is normally to combine MRAC with other structures in order to guarantee the system performance, to reduce the unknown model dynamics, disturbances, to have a better transient behavior, etc. It is important to remark that the Lyapunov theory implemented to design the MRAC guarantees closed-loop stability with also fault-tolerant capabilities.

REFERENCES

Abdal, F., Abbas, R., and Abdulsada, M. A. (2010). Simulation of wind-turbine speed control by matlab. *International Journal of Computer and Electrical Engineering*, 2(5):912–915.

Abdin, E. and Xu, W. (2000). Control design and dynamic performance analysis of a wind turbine-induction generator unit. *IEEE Transactions on Energy Conversion*, 15(1):91–96.

Astrom, K. and Wittenmark, B. (1995). *Adaptive Control*. Addison-Wesley Publishing Company, 2nd edition.

Carter, R., Cruden, A., Hall, P., and Zaher, A. (2012). An improved lead acid battery pack model for use in power simulations of electric vehicles. *IEEE Transactions on Energy Conversion*, 27(1):21–28.

Chiasson, J. and Vairamohan, B. (2005). Estimating the state of charge of a battery. *IEEE Transactions on Control Systems Technology*, 13(3):465–470.

Fuchs, E. F. and Masoum, M. A. (2011). Analyses and designs related to renewable energy systems. In *Power Conversion of Renewable Energy Systems*, pages 557–687. Springer US.

Fusco, G. and Russo, M. (2008). Adaptive voltage regulator design for synchronous generator. *IEEE Transactions on Energy Conversion*, 23(3):946–956.

Fusco, G. and Russo, M. (2012). Nonlinear control design for excitation controller and power system stabilizer. *Control Engineering Practice*, 19(3):243–251.

Gentile, T. J. (2009). Smart grid a necessary component in the remaking of america. *IEEE-USA Annual Meeting*.

Hiyama, T. (2011). *Intelligent Automatic Generation Control*. CRC-Press.

Jiang, Z., Li, F., Qiao, W., Sun, H., Wan, H., Wang, J., Xia, Y., Xu, Z., and Zhang, P. (2009). A vision of smart transmission grids. pages 1–10.

Jugo, J. (2002). Discretization of continuous time-delay systems. In *Proceedings of the 15th IFAC World Congress, 2002*, pages 117–122.

Kassem, A. M. (2012). Robust voltage control of a stand alone wind energy conversion system based on functional model predictive approach. *International Journal of Electrical Power and Energy Systems*, 41:124–132.

Kassem, A. M. and Ali, M. Y. (2011). Robust control of an isolated hybrid winddiesel power system using linear quadratic gaussian approach. *International Journal of Electrical Power and Energy Systems*, 33:1092–1100.

Kini, A. and Yaragatti, U. (2006). Modelling and simulation of a wind/diesel hybrid power system. In *Proceedings of the IEEE International Conference on Industrial Technology, ICIT*, pages 1670–1675.

Kuang, B., Wang, Y., and Tan, Y. L. (2000). An h_∞ controller design for diesel engine systems. In *Proceedings of the International Conference on Power System Technology*, volume 1, pages 61–66.

Kumar, B., Mishra, S., Bhende, C., and Chauhan, M. (2008). Pi controller based frequency regulator for distributed generation. In *Proceedings of the TENCON - IEEE Region 10th Conference*, pages 1 –6.

Lee, S.-H., Yim, J.-S., Lee, J.-H., and Sul, S.-K. (2008). Design of speed control loop of a variable speed diesel engine generator by electric governor. pages 1–5.

Minchala, L., Garza, L., and Calle, E. (2012). An intelligent control approach for designing a low voltage dc breaker. Number 4, pages 163–166.

Munoz-Aguilar, R., Doria-Cerezo, A., Fossas, E., and Cardoner, R. (2011). Sliding mode control of a standalone wound rotor synchronous generator. *IEEE Transactions on Industrial Electronics*, 58(10):4888–4897.

Nagrath, I. and Gopal, M. (2008). *Control Systems Engineering*. Anshan Ltd Press, United Kingdom., 5th edition.

Schwaegerl, L., Tao, J.P.; Lopes, A., Madureira, P., Mancarella, A., Anastasiadis, N., Hatziargyriou, and Krkoleva, A. (2009). Report on the technical, social, economic, and environmental benefits provided by microgrids on power system operation.

Vandoorn, T., Meersman, B., Degroote, L., Renders, B., and Vandevelde, L. (2011). A control strategy for islanded microgrids with dc-link voltage control. *IEEE Transactions on Power Delivery*, 26(2):703–713.

Vechiu, I., Camblong, H., Tapia, G. B., and Dakyo, C. N. (2004). Dynamic simulation model of a hybrid power system: Performance analysis. *2004 European Wind Energy Conference*.

Wang, L. (2009). *Model Predictive Control System Design and Implementation Using MATLAB*. Springer Publishing Company, Incorporated, 1st edition.

Zeng, L. and Hu, G.-D. (2010). Discretization of continuous-time systems with input delays. *Acta Automatica Sinica*, 36(10):1426–1431.